DOI: 10.13009/EUCASS2017-94

A Study on Missile Autopilot Design using Nonlinear Adaptive Sliding Mode Control Scheme

*Gwanyoung Moon * and Yougwoo Lee ***
** Agency for Defense Development*
Sunamdong Yousunggu Daejeon, Republic of Korea
*** Agency for Defense Development*
Sunamdong Yousunggu Daejeon, Republic of Korea

Abstract
The nonlinear control scheme generally uses the cancellation or inversion process based on the exact system identification. However, the external disturbances as well as unknown system characteristics degrade the control system performance. To cope with these uncertainties, in this paper, the adaptive sliding mode control scheme is adopted with nonlinear back-stepping autopilot structure similar to the novel 3 loop controller. Firstly the basic control structure is introduced and advanced compensation terms are added. The system performance is evaluated with some numerical simulations.

1. Introduction

One of the important performance factor required for the intercepting ballistic target is the autopilot swiftness of the intercepting missile. By introducing the nonlinear control theory, the autopilot performance can be improved. In this reason the nonlinear control technique has been widely investigated for designing fast autopilot.[1-3] Many previous papers has been researched for suggest new the nonlinear controllers. Nevertheless analytical approaches used in nonlinear control theory give some abstract ideas about the stable region; Most of them just suggest range or bound for satisfying stability. However, choosing proper gain is very essential part in applying the nonlinear control in real world. In previous work, to solve this problem, MDO(Multi-Disciplinary Optimization) concept is researched.
Meanwhile, the nonlinear control uses much information compared to linear control system; this makes the nonlinear controller have a weakness in robustness. To overcome these shortcomings, there are several attempts using linear and nonlinear technique. Among them, most prominent approach is the sliding mode control technique. Sliding mode control uses sliding surface as a sliding manifold; the signal outside the surface generates additional inputs and once the state locates on the surface, the control input keeps the states stay at the surface. This too powerful control scheme induces the chattering phenomenon in general sliding mode control.
In this paper, design of nonlinear autopilot based on back-stepping theory is addressed with optimal control gain. Using developed MDO environment the nonlinear control gain is obtained. Adaptive sliding mode control structure is also proposed. Even in the adaptive sliding mode control, it has gain to be set. Analogues between back-stepping control and sliding mode control give a clue to formulate the sliding surface. And to reduce the excess input adaptive law for the control gain is used. After basic theoretic explanation, numerical simulation is performed to check the validity of proposed algorithm.

2. Design Autopilot using Back-stepping Technique

2.1 System dynamics

The rigid body translational equations of motion are represented as

$$\frac{X}{m} + g_x = \dot{u} + qw - rv \quad \textbf{(1)}$$

$$\frac{Y}{m} + g_y = \dot{v} + ru - pw \quad \textbf{(2)}$$

$$\frac{Z}{m} + g_z = \dot{w} + pv - qu \quad \textbf{(3)}$$

DOI: 10.13009/EUCASS2017-94

where, *u*, *v*, and *w* is missile velocity in body frame, respectively. The angular rate is expressed in *p*, *q*, *r*; it means roll, pitch, yaw rate sequentially. *X*, *Y* and *Z* mean external forces and m is a mass of the missile. Three angular rate and accelerations can be obtained directly from gyros and accelerometers in IMU system. g_x, g_y and g_z are gravity accelerations. For the rotational dynamics of axis-symmetric cruciform missile, following equations are used for simplicity

$$L = I_{xx}\dot{p} \tag{4}$$
$$M = I_{yy}\dot{q} + rp(I_{xx} - I_{zz}) \tag{5}$$
$$N = I_{zz}\dot{r} + pq(I_{yy} - I_{xx}) \tag{6}$$

where, *L*, *M* and *N* represent external moment. I_{xx} , I_{yy} and I_{zz} are major axis moment of inertia. The external force and moment are defined as

$$X = -QS(C_{x0} + C_x^{Base} + C_{x\delta}) \tag{7}$$
$$Y = QS(C_{y0} + C_{y\delta}) \tag{8}$$
$$Z = QS(C_{z0} + C_{z\delta}) \tag{9}$$
$$L = QSD(C_{l0} + C_{l\delta}) + \frac{QSD^2}{2V_T}C_{lp}p \tag{10}$$
$$M = QSD(C_{m0} + C_{m\delta}) + \frac{QSD^2}{2V_T}C_{mq}q \tag{11}$$
$$N = QSD(C_{n0} + C_{n\delta}) + \frac{QSD^2}{2V_T}C_{nr}r \tag{12}$$

where, C_{x0}, C_{y0}, C_{z0}, C_{l0}, C_{m0}, C_{n0} indicate the basic non-dimensional aerodynamic coefficients; These are functions of Mach, altitude, total angle of attack, and aerodynamic bank. $C_{x\delta}$, $C_{y\delta}$, $C_{z\delta}$, $C_{l\delta}$, $C_{m\delta}$, $C_{n\delta}$ denote aerodynamic coefficients related to the control input. C_{lp}, C_{mq}, C_{nr} represent aerodynamic damping terms for each channel. *Q* means a dynamic pressure. S and D correspond to cross-sectional area and reference length, respectively, and V_T denote a total velocity.

If the longitudinal dynamics is considered only, the above equations can be simplified as followings

$$\dot{a}_z = \frac{Qs}{m}\left(C_{z_\alpha}\dot{\alpha} + C_{z_\beta}\dot{\beta} + C_{z_{\delta_p}}\dot{\delta}_p\right) \tag{13}$$
$$\dot{q} = \frac{1}{I_{yy}}\left\{QSD(C_{m0} + C_{m\delta}) + \frac{QSD^2}{2V_T}C_{mq}q - rp(I_{xx} - I_{zz})\right\} \tag{14}$$

where α, β represent angle of attack, and side slip angle, respectively.

2.2 Back-stepping control technique

The acceleration is a major state for describing the missile status. And more, the proportional navigation guidance law generates the acceleration command for the inner autopilot loop. In this reason, the classical 3 loop control system is composed with the acceleration feed-back loop as the exterior part of the overall autopilot system. Suppose the acceleration loop is controlled with the first order

$$\dot{a}_z = K_a\left[a_{zc} - a_z\right] \tag{15}$$

where, a_{zc} means acceleration command and K_a is acceleration control gain. And the first derivative of angle of attack and side slip angle is shown

$$\dot{\alpha} = q - (pcos\alpha + rsin\alpha)tan\beta + \frac{1}{mVcos\beta}(F_z cos\alpha - F_x sin\alpha) \tag{16}$$
$$\dot{\beta} = psin\alpha - rcos\alpha + \frac{1}{mV}\left(-F_x cos\alpha sin\beta + F_y cos\beta - F_z sin\alpha sin\beta\right) \tag{17}$$

Now combining equations from Eq.(13) to Eq.(17), the pitch angular rate command is computed as following

$$q_c = K_a\frac{m}{QsC_{z_\alpha}}\left(a_{zc} - a_z\right) - \dot{\alpha} - \frac{C_{z_\beta}}{C_{z_\alpha}}\dot{\beta} + q \tag{18}$$

DOI: 10.13009/EUCASS2017-94

Meanwhile, for the case that the slope of pitch moment according to the fin deflection is not affected, Eq. (14) can be rewritten as

$$\dot{q} = \frac{1}{I_{yy}}\left\{QSDC_{m0} + \frac{QSD^2}{2V_T}C_{mq}q - rp(I_{xx} - I_{zz})\right\} + \frac{QSD}{I_{yy}}C_{m_\delta}\delta_p \quad \textbf{(19)}$$

With Eq.(19), the pitch dynamics is expressed with an input-affine form. With help of this equation the control input can be derived explicitly. Now we can move to the inner loop of autopilot system; the pitch rate loop is applied to a proportional-derivative type controller

$$\dot{q} = K_r\left(e_q + K_i\int e_q\right) \quad \textbf{(20)}$$

where, e_q means the error between pitch and its desired rate which comes from outer acceleration loop. K_r, K_i are control gain, respectively. Now cumulating equations from Eq.(18) to Eq.(20) gives the control fin

$$\delta_p = \frac{1}{g_m}\left[-f_m + \frac{1}{Qsd}\left\{I_{yy}K_r\left(e_q + K_i\int e_q\right) + rp(I_{xx} - I_{zz})\right\}\right] \quad \textbf{(21)}$$

where, f_m, g_m is defined as following

$$f_m = C_{m0} + \frac{D}{2V_T}C_{mq}q \quad \textbf{(22)}$$

$$g_m = C_{m_\delta} \quad \textbf{(23)}$$

Note the control input has three design parameters: K_a, K_i, and K_r. This is almost same structure compared to the classical 3 loop autopilot system. These gains should be carefully designed although their affection is not so severe compared to the classical 3 loop controller.

2.3 Autopilot gain optimization

The proposed back-stepping nonlinear autopilot has three parameters to be determined. These control gain should satisfy the stability and performance criterion. However, for the non-linear control system, there is no common standard to evaluate the stability margin in the frequency domain; Most of them are too complicate or improper to apply directly autopilot design process. For the above reason, time domain response is taken as a major index for evaluating the performance and stability of proposed nonlinear algorithm.

In order to find the nonlinear control gain, the optimization process is utilized in this paper. Choosing a proper performance index and constraints is an essential factor for the optimization. As a performance index for the control gain, the rise time of a step response is considered. Since achieving a fast response of the missile is one of the most important virtues in autopilot design. And the overshoot of acceleration loop is also taken as a cost function. Including this index may sacrifice the fast rise time performance, but considering overshoot takes a part of stability margin in nonlinear time domain response. While minimizing these performance indices, several constraints can be taken into account. In this problem, the time response of the acceleration loop under 6DOF circumstance is considered as a constraint.

As an optimization engine, the modeFRONTIER is used. It is a supervising program for composing the multi-disciplinary design optimization environment; by using this tool, it is possible to combine several useful programs such as visual studio, MATLAB and so on. In figure 1 shows one example of the optimization environment used for obtaining the optimal control gain set.

DOI: 10.13009/EUCASS2017-94

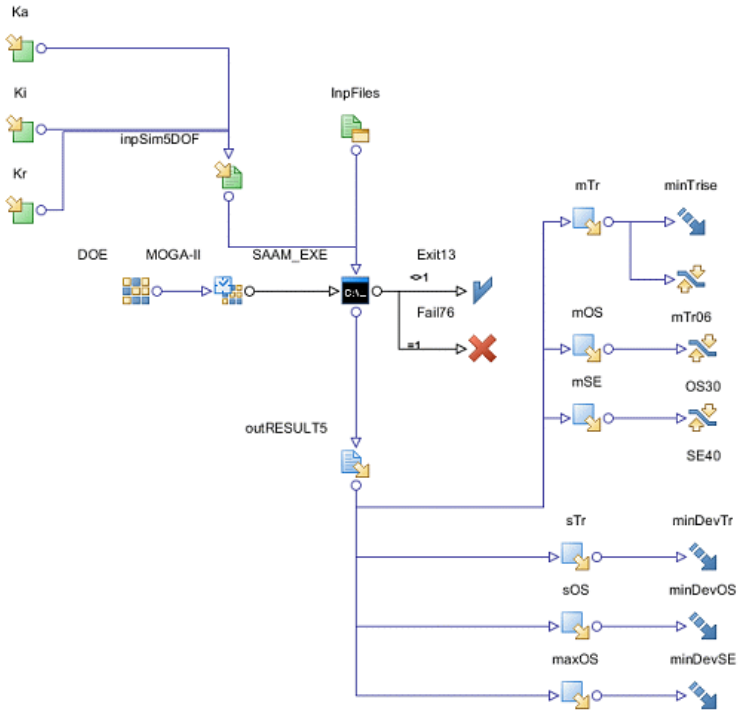

Figure 1: Developed optimization environment example

3. ADAPTIVE SLIDING MODE CONTROL DESIGN

3.1 Sliding mode control design

Let's consider following sliding mode surface

$$S_q = s_3(q_c - q) + s_4 \int (q_c - q) \tag{24}$$

Differentiating above equation with time results

$$\dot{S_q} = s_3(\dot{q_c} - \dot{q}) + s_4 \int (\dot{q_c} - \dot{q}) \tag{25}$$

Suppose the sliding surface holds following equation

$$\dot{S_q} = k_s S_q + k_e sign(S_q) \tag{26}$$

Prop1. The sliding surface S_q in Eq.(24) keeps the sliding manifold with Eq.(26)
Prof) Let's consider following positive definite function as Lyapunov function

$$V = \frac{1}{2} S_q^2 \tag{27}$$

The first time derivative of Eq.(27) gives

$$\dot{V} = S_q \, \dot{S_q} \tag{28}$$

Now, inserting the Eq.(26) into Eq. (28) results

$$\dot{V} = k_s S_q^2 + k_e sign(S_q) S_q \tag{29}$$

DOI: 10.13009/EUCASS2017-94

If $k_s < 0$, $k_e < 0$ are hold, the first derivative of Lyapunov function is always negative definite. Therefore, the sliding surface Eq.(24) holds its sliding manifold.■

Interconnecting Eq.(25) and Eq.(26) obtains

$$s_3(\dot{q}_c - \dot{q}) + s_4 \int (\dot{q}_c - \dot{q}) = k_s S_q + k_e sign(S_q) \quad \textbf{(30)}$$

If the sliding surface is designed with $S_3 \neq 0$, then Eq.(30) can be rearranged as following.

$$\dot{q} = \dot{q}_c + \frac{s_4}{s_3}(q_c - q) - \frac{k_s}{s_3} S_q - \frac{k_e}{s_3} sign(S_q) \quad \textbf{(31)}$$

Now, using the pitch rate equation in Eq.(5), the pitch moment can be explicitly expressed as

$$M = I_{yy}\left\{\dot{q}_c + \frac{s_4}{s_3}(q_c - q) - \frac{k_s}{s_3} S_q - \frac{k_e}{s_3} sign(S_q)\right\} + rp(I_{xx} - I_{zz}) \quad \textbf{(32)}$$

Consequently, the control input can be computed

$$\delta_p = \frac{1}{g_m}\left[-f_m + \frac{I_{yy}}{Qsd}\left\{\frac{s_4}{s_3}(q_c - q) - \frac{k_s}{s_3} S_q - \frac{k_e}{s_3} sign(S_q)\right\} + \frac{rp}{Qsd}(I_{xx} - I_{zz})\right] \quad \textbf{(33)}$$

Next, the sliding mode control gain should be found. Before proceeding to seek the sliding gain, note that we already have an optimal control gain set for the similar nonlinear control structure. Observing the resulting sliding mode control input, it is easily found that except the sign function augmented term, every term has a matching element in basic nonlinear control input shown in Eq.(21). Consequently, there should be some relationship between the previous optimal gain and the sliding mode control gain. Concentrating on the similarity Eq.(21) and Eq.(33) leads

$$\frac{s_4}{s_3} - k_s = K_r \quad \textbf{(34)}$$

$$-k_s \frac{s_4}{s_3} = K_i K_r \quad \textbf{(35)}$$

To specify the sliding mode control gain, solving simultaneous equations gives

$$k_s^2 + K_r k_s + K_i K_r = 0 \quad \textbf{(36)}$$

Therefore the sliding mode control gain can be as

$$k_s = \frac{-K_r - \sqrt{K_r^2 - 4K_i K_r}}{2} \quad \textbf{(37)}$$

$$s_3 = 1 \quad \textbf{(38)}$$

$$s_4 = -\frac{K_i K_r}{k_s} \quad \textbf{(39)}$$

Because, $k_s \neq 0$ should be kept, a negative solution candidate is selected for the gain k_s. With these relationships, the sliding mode control without a sign function augmented term, has the same property with basic nonlinear control law.

3.2 Design adaptive sliding gain

The control gain k_e makes the proposed control system have sliding mode property; with non-zero k_e, the proposed controller forces states to the sliding surface that is a sliding manifold. This term however exerts negative effect on the system so called chattering phenomenon or unanticipated oscillation like to the high gain application. To alleviate this phenomenon, the adaptive sliding mode control technique is proposed; once the state stays on the sliding surface, then the driving additional effect is diminished. So as to satisfy this purpose, the sliding mode gain shown In Eq.(26) is set as following

DOI: 10.13009/EUCASS2017-94

$$k_e = \begin{cases} -\Lambda & (\Lambda < k_{ad}) \\ -k_{ad} & (0 < k_{ad} < \Lambda) \\ 0 & (k_{ad} < 0) \end{cases} \quad \textbf{(40)}$$

where, the parameter k_{ad} is determined by following adaptive law

$$\dot{k}_{ad} = \begin{cases} -\sigma & (|S_q| < \dot{o}_\sigma) \\ \xi |S_q| & (|S_q| \geq \dot{o}_\sigma) \end{cases} \quad \textbf{(41)}$$

where, Λ, σ, ξ and, ε_σ are all positive constants. Making good use of a proper adaptive constant, the proposed sliding mode control structure generates an additional control input to drive the states in the sliding manifold with quick. It is derived to decrease this extra input after satisfying the purpose of control; This also prohibit the build-up control signal from chattering around sliding manifold after reaching the surface.

Prop 2. For $|S_q| \geq \varepsilon_\sigma$, the proposed adaptive system makes the state converge to the sliding surface S_q exponentially.

Prof) Differentiating the sliding surface manifold written in Eq.(26) gives

$$\ddot{S}_q = k_s \dot{S}_q - \xi |S_q| sign(S_q) \quad \textbf{(42)}$$

This equation can be rewritten as following

$$\ddot{S}_q - k_s \dot{S}_q + \xi S_q = 0 \quad \textbf{(43)}$$

Therefore the sliding surface S_q has two eigenvalues :

$$\lambda_{S_q} = \frac{k_s \pm \sqrt{k_s^2 - 4\xi}}{2} \quad \textbf{(44)}$$

One should note that $k_s < 0$ induces the time domain solution to converge exponentially if the deterministic equation is negative. Even for the positive deterministic equation case, the convergent property is hold since $\xi > 0$; $k_s^2 > k_s^2 - 4\xi$ is always satisfied. In this reason, the sliding surface S_q converges exponentially. ■

In the view point of control input, the augmented input invoked by the sign function can be explained as a local maximum control force is provided to the system for fast decreasing of off-set signals into the sliding manifold. This enables the sliding mode control to regulate disturbances and reject uncertainties. If the states arrive to the sliding manifold, that is $|S_q| < \varepsilon_\sigma$, decreasing of extra input except maintaining the sliding surface input will be helpful to cope with next un-expected circumstances.

4. NUMERICAL SIMULATION EXAMPLE

4.1 Basic back-stepping control example

The suggested control structure starts from the basic back-stepping control. Except the sign function term, all control gain is determined by the basic nonlinear control gain. To find the nonlinear optimal gain, the developed multi-disciplinary optimization environment is used. In this environment, three cost functions are considered; it generates an optimal gain Pareto curve shown in figure 2.

Among these candidate gain set, an optimal control gain set can be chosen by considering the gain continuity of adjacent scheduling design points and design purpose. Figure 3 displays the step response of back-stepping nonlinear autopilot with optimal gain. Upper diagram explains the response of major axis response of close loop system, and lower figure shows minor axis response. In major axis response, the rising time is read under 0.2sec without excess

DOI: 10.13009/EUCASS2017-94

overshoot. In classical 3 loop control case the minor axis response was a big issue. The coupling signal with major response was inevitable, but the proposed back-stepping scheme regulates this parasitic maneuver almost under 1G level as shown in figure 3.

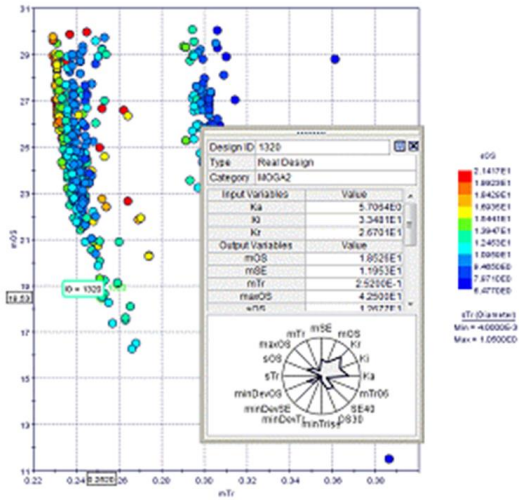

Figure 2: Sample Pareto curve for back-stepping control

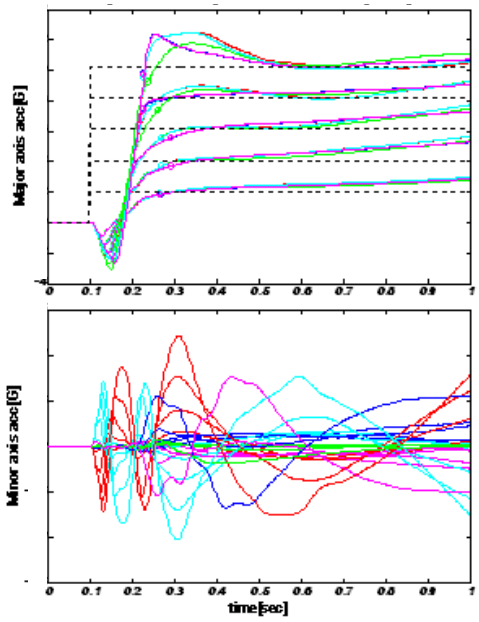

Figure 3: Basic nonlinear controller response

4.2 Adaptive sliding mode control example

To check and evaluate the performance of proposed algorithms, a programmed command scenario is tested under several different conditions. Firstly, under a normal condition, numerical simulations are performed for the 3-loop linear controller, the basic back-stepping control and the proposed adaptive sliding mode control, respectively. As we expected, in an ideal environment, the proposed nonlinear controllers show better performance compared to the linear one as shown in Fig 4. The main reason for the degradation in off-axis is that the linear control system does not consider the aerodynamic bank angle as a slack variable.

Figure 5 represents the result of external wind is applied to the 6DOF nonlinear simulation. Compared to the previous result, the performance of the basic back-stepping control is a little degraded. The nonlinear controllers use the information of angle of attack and side slip angle; this makes the nonlinear controller superiority to classical one. Ironically, the main reason for the performance deterioration in the windy environment is identical; the erroneous using of aero-based data degrades the nonlinear control performance.

Nonetheless, the adaptive sliding mode control reduces this declination by the help of the additional driving input invoked by the sign function. Note the classical controller has same performance even in the windy disturbance circumstance.

5. CONCLUSION

The nonlinear control based on the back-stepping technique with optimal gain is proposed. The control gain is optimized by using multi-disciplinary optimization environment. To enforce the performance of suggest nonlinear autopilot, the adaptive sliding mode concept is adopted. So as to use the existing optimal nonlinear gain, the relation between back-stepping gain and sliding surface parameter is explored. The efficiency of suggested autopilot is evaluated by numerical simulations for a sample case. In nominal case, the performance of nonlinear controller is superior to the classical one. In a disturbance environment, the degradation is not evitable; however, the proposed adaptive sliding mode control lessens this weakness in nonlinear structure.

DOI: 10.13009/EUCASS2017-94

References

[1] Plestan, F., Shtessel, Y., Bregeault, V., and Poznyak, A., "New Methodologies for Adaptive Sliding Mode Control," International Journal of Control, Vol.83, No.9, 2010, pp.1907-1919.

[2] Polycarpou, M. M., and Ioannou, P. A., "A Robust Adaptive Nonlinear Control Design," Automatica, Vol.32, No.3, 1996, pp.423-427.

[3] Freeman, R. A., Krstic, M., and Kokotovic, P. V., "Robustness of Adaptive Nonlinear Control to Bounded Uncertainties," Automatica, Vol.34, No.10, 1998, pp.1227-1230.

[4] Seibert, P., and Suarez, R., "Global Stabilization of Nonlinear Cascade Systems," System & Control Letters, Vol.14, No.4, 1990, pp.347-352.

[5] Isidori, A., Nonlinear Control System, Springer-Verlag, Berlin, 1989.

[6] Chakraborty, A., Seiler, P., and Balas, G. J., "Nonlinear Region of Attraction Analysis for Flight Control Verification," Control Engineering Practice, Vol.19, No.4, 2011, pp.335-345.

[7] Wang, Q., and Stengel, R.F., "Robust Nonlinear Control of a Hypersonic Aircraft," Journal of Guidance, Control, and Dynamics, Vol.23, No.4, 2000, pp.577-585.

[8] Wang, Q., and Stengel, R.F., "Robust Control of Nonlinear Systems with Parametric Uncertainty," Automatica, Vol.38, No.9, 2002, pp.1591-1599.

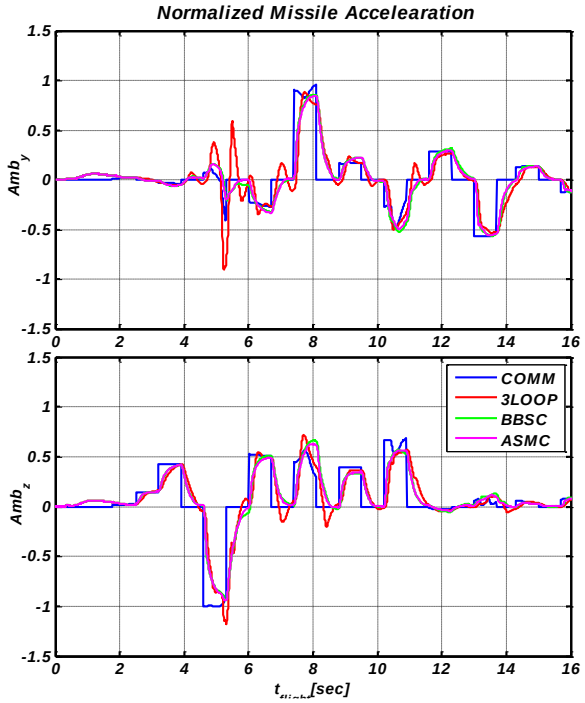

Figure 4: Normalized Acceleration Response (No wind)

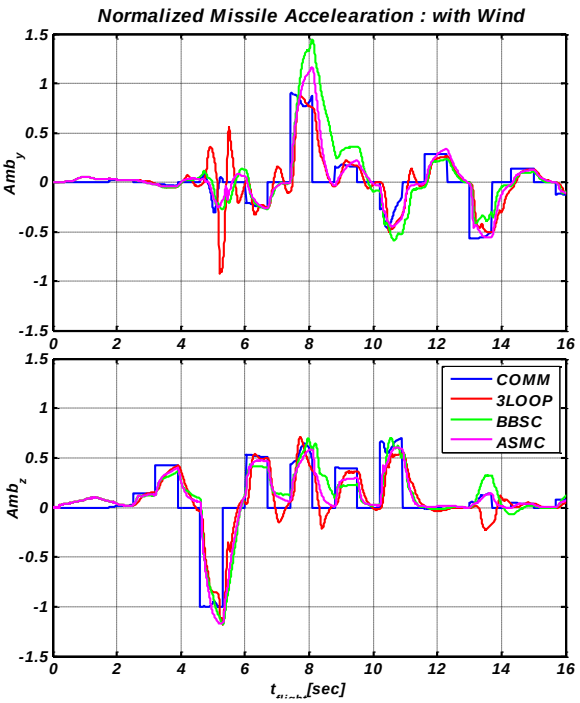

Figure 5: Normalized Acceleration Response (Wind)